

Quasi-Resonant Full-Wave Zero-Current Switching Buck Converter Design, Simulation and Application

G. Yanik and E. Isen

Abstract—This paper presents a full wave quasi-resonant zero-current switching buck converter design, simulation and application. The converter control uses with zero-current switching (ZCS) technique to decrease the switching losses. Comparing to conventional buck converter, resonant buck converter includes a resonant tank equipped with resonant inductor and capacitor. The converter is analyzed in mathematical for each subintervals. Depending on the desired input and output electrical quantities, converter is designed with subinterval equations. The converter is simulated in PSIM with design parameters. The simulation results are verified with experimental setup. The converter is controlled by UC3867N integrated resonant mode power supply controller.

Index Terms—Buck converter, resonant converter, zero current switching,

I. INTRODUCTION

THE switching frequency or output filter components values must be increased to improve the output performance of conventional hard switching PWM DC-DC converters. Increased switching frequency causes increase in switching losses and electromagnetic noise. Furthermore, more losses cause warming problems, thus bigger heat sink or higher current capacity switching device usage is needed. To solve the problems occurs during switching zero-current switching (ZCS) and zero-voltage switching (ZVS) techniques have been improved [1]-[3]. Using a series connected inductor and a parallel connected capacitor to switching device ZCS and ZVS techniques can be applied [4]. In addition, these soft switching techniques can be applied with resonant circuits [5]. The switch current is decreased to zero with resonant, and then switching signal is off to turn-off the switching device. Thus, switching loss could be significantly decreased with ZCS. In ZVS technique, the voltage on the switch is forced to be zero with resonant before turn-on. When the current decreases to zero, switching signal is applied to turn-on the switch. Hence, the loss occurs during the turn-on greatly decreased [6].

G. YANIK, is with the Electrical Engineering Department, Electrical & Electronics Faculty, Yildiz Technical University, Istanbul, 34220, TURKEY. (e-mail: gyanik@yildiz.edu.tr).

E. ISEN, is with the Electrical & Electronics Engineering Department, Engineering Faculty, Kırklareli University, Kırklareli, TURKEY. (e-mail: evren.isen@kirkclareli.edu.tr).

Soft switching techniques are mostly used in DC-DC converters, such as buck converter, boost converter [7],[8]. The placed resonant circuit between output filter and input source is utilized to force the current and voltage to become zero. The resonant circuits are classified in three categories, conventional, quasi-resonant and multi-resonant.

Quasi-resonant converters can be performed as half-wave [9] and full-wave [10]. Considering the quasi-resonant buck converter, conventional buck converter can be worked with resonant by connecting a series inductor to the switch utilized in the input and a parallel capacitor to the output diode. While a unidirectional switching device is used in half-wave quasi-resonant converter, bidirectional switching device is used in full-wave quasi-resonant converter. Operating principle is the same for both converters. However, reverse inductor current can flow through the anti-parallel diode of switch, thus resonant interval increases. Therefore, this condition lets resonant energy be transferred back to input source in low load operating, and the dependence of output voltage to the load decreases. As a result, use of quasi-resonant converter instead of conventional DC-DC converter provides low switching losses, high efficiency, ability of working in higher frequencies, low EMI and low value of output filter elements.

In this study, 60 W quasi-resonant full-wave (QRFW) zero-current switching (ZCS) buck converter is analyzed, simulated and implemented. Operating intervals of the converter are examined, circuit equations for each interval are derived and circuit parameters are calculated. The converter is simulated with calculated parameters and the simulation results are verified with experimental results.

II. SERIES RESONANT CIRCUITS

In this section, operating principle of series resonant circuits is explained to understand quasi-resonant full-wave converter operating. As shown in Fig. 1, series resonant circuit includes series connected an inductor and a capacitor. When the input voltage is applied to resonant circuit, a resonant occurs between these resonant elements. Circuit equations during the resonant are given in (1)-(3) and waveforms are shown Fig. 2.

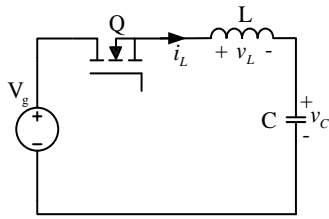


Fig. 1. Series resonant circuit

$$i_L = I_{L0} \cos \omega t + \frac{V_g - V_{C0}}{Z} \sin \omega t \tag{1}$$

$$V_L = (V_g - V_{C0}) \cos \omega t - ZI \sin \omega t \tag{2}$$

$$V_C = -(V_g - V_{C0}) \cos \omega t + ZI_{L0} \sin \omega t + V_g \tag{3}$$

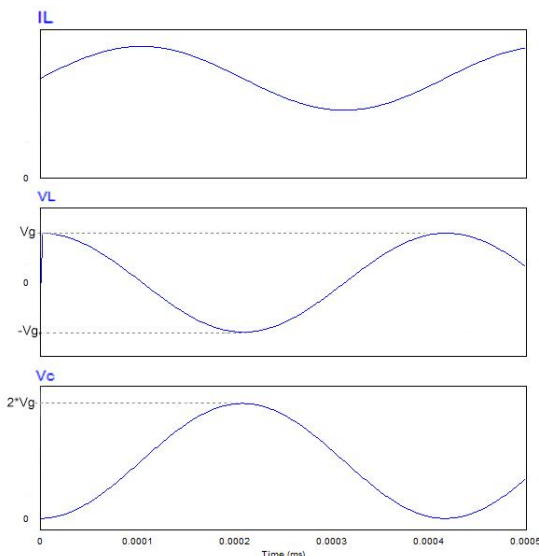


Fig. 2. Series resonant circuit waveforms

III. THEORETICAL ANALYSIS

QRFW buck converter is a special version of the traditional buck converter that uses resonant intervals to ensure soft switching of the semiconductor device. In this section, operation principle of the QRFW buck converter that is shown in Fig. 3 along with subintervals of the converter will be analyzed.

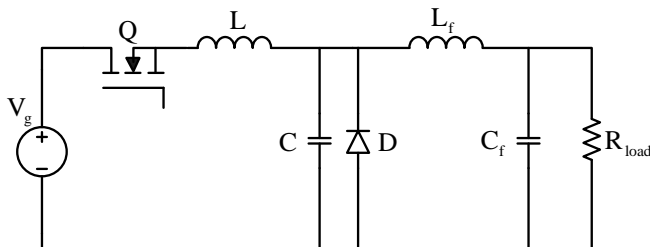


Fig. 3. Full Wave Quasi Resonant Buck Converter Topology

Before subinterval 1, converter is assumed to be working in steady state. Inductor current and output voltage are set to nominal values. The output diode D conducts the filter inductor current I_{Lr} . Filter inductor is assumed to be so large

that output current I_{Lf} is constant during one switching cycle. Subinterval 1 starts with the signal applied to the switch Q.

A. Subinterval 1

The switch Q turns on and input voltage V_g is applied to the resonant inductor L. Therefore, resonant inductor current rises linearly, with the slope of V_g/L and diode current decreases from I_{Lf} to zero, with the same slope. Switch current increases linearly with a slightly slow slope, therefore ZCS turn on of the switch is provided. Fig. 4 shows the subcircuit in this interval.

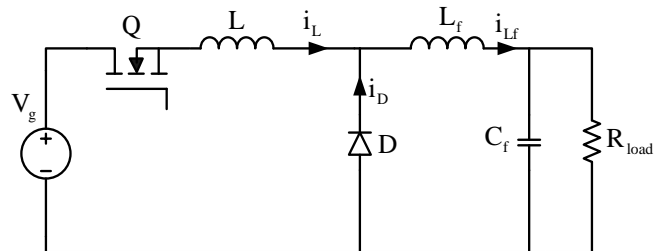


Fig. 4. Subcircuit in subinterval 1

$$I_L = \frac{V_g}{L} t \tag{4}$$

$$V_C = 0 \tag{5}$$

When resonant inductor current reaches to I_{Lf} and the diode turns off, this interval ends.

B. Subinterval 2

Fig. 5 shows the subcircuit in this interval. In the input side of the converter, a series resonant tank occurs where L and C are the resonant elements.

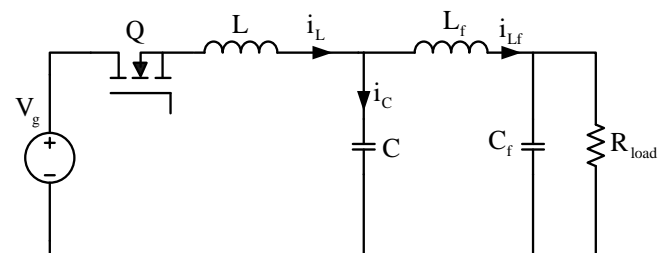


Fig. 5. Subcircuit in subinterval 2

Resonant inductor has initial current I_{Lf} and inductor current continues to increase in sinusoidal. Resonant capacitor voltage also starts to increase, simultaneously. Related state equations can be calculated from (1) and (3).

$$I_L = I_{L0} + \frac{V_g}{Z} \sin \omega t \tag{6}$$

$$V_C = V_g - V_g \cos \omega t \tag{7}$$

When inductor current decreases to zero, this interval ends.

C. Subinterval 3

Fig. 6 shows subcircuit in this interval. As it is seen in the figure, the subcircuit is the same with the previous subinterval but resonant inductor and resonant capacitor currents are reversed.

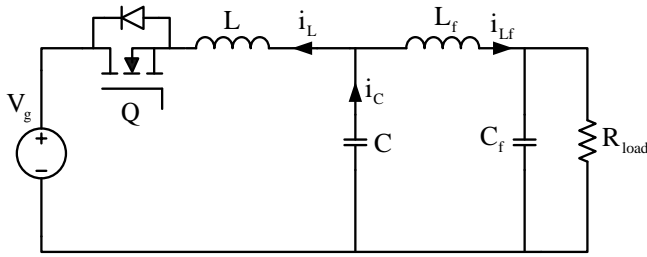


Fig. 6. Subcircuit in subinterval 3

In the beginning of this interval, a negative ringing between resonant elements starts. Resonant current flows through the body diode of the switch. This is the ZCS interval where control signal applied to the switch must be cut off to ensure turn the switch off with ZCS. State equations of the resonant elements are the same with the previous one and given below.

$$I_L = I_{Lf} + \frac{V_g}{Z} \sin \omega t \tag{8}$$

$$V_C = V_g - V_g \cos \omega t \tag{9}$$

This interval ends when resonant current reaches to zero.

D. Subinterval 4

The subcircuit of this interval is shown in Fig. 7. At the start of this interval, resonant capacitor is not discharged completely therefore, output current I_{Lf} flows through resonant capacitor, discharging it linearly with the slope of I_{Lf}/C .

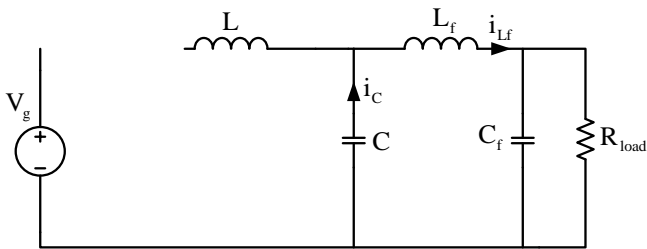


Fig. 7. Subcircuit in subinterval 4

State equations of the resonant elements are given below.

$$I_L = 0 \tag{10}$$

$$V_C = \frac{I_{Lf}}{C} \tag{11}$$

This interval ends when capacitor voltage decreases to zero and output diode turns on.

E. Subinterval 5

When capacitor voltage decreases to zero, output inductor

current turns on the diode. Corresponding subcircuit is shown in Fig. 8. This subinterval is the off state of the traditional converter. Output current is conducted by the diode and this interval ends when the switch is back on. Unlike the traditional buck converter, this subinterval is the control interval. In the traditional buck converter, duration of the on state of the switch controls output voltage. In QRFW buck converter, off stage duration is adjusted to control the output voltage. Therefore, the on time of the switch is constant and defined by the resonant elements.

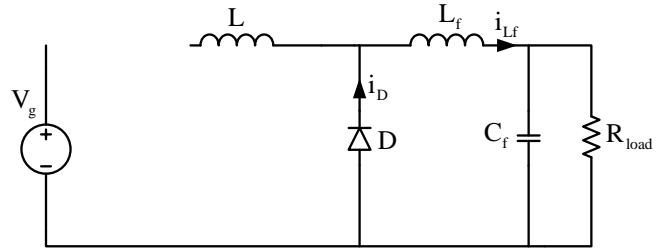


Fig. 8. Subcircuit in subinterval 5

Theoretical waveforms of the resonant tank are shown in Fig. 9.

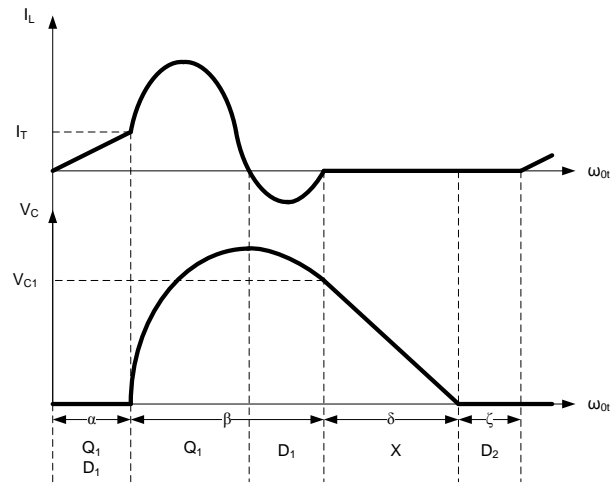


Fig. 9. Theoretical waveforms of the resonant tank

IV. DESIGN CONSIDERATION

To design any SMPS circuit, output power, input and output voltages and switching frequency must be considered. These parameters of the designed converter are shown in TABLE I.

TABLE I
DESIGN CONSIDERATION

Symbol	Quantity	Value
P_o	Output power	60 W
V_g	Input voltage	48 V
V_o	Output voltage	12 V
f_s	Switching frequency	200 kHz

In a QR converter, values of the resonant elements are crucial for the operation. In this section, selections of the resonant elements are explained.

In the second interval of the converter, a series resonant circuit tank, loaded with a current source, occurs as shown in Fig. 10.

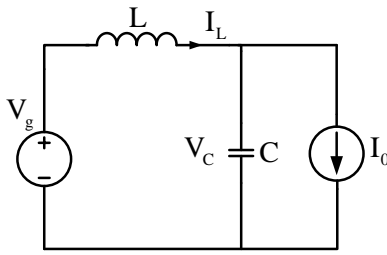


Fig. 10. Series resonant tank loaded with constant current source

In this resonant circuit, resonant inductor current is calculated as below.

$$I_L = I_o + \frac{V_g}{\sqrt{\frac{L}{C}}} \sin \omega t \tag{12}$$

In a QRFW buck converter, current source value must be lower than resonant current peak level to ensure negative ringing, where switch signal will be cut off. Output current is selected as 5 Amps due to the output power and voltage. Therefore, resonant tank current must be greater than 5.

$$I_{Lres(peak)} > 5 \tag{13}$$

$$I_o = \frac{V_g}{\sqrt{\frac{L}{C}}} \sin \omega t \Rightarrow 5 = \frac{12}{\sqrt{\frac{L}{C}}}; \sqrt{\frac{L}{C}} > 2.4 \tag{14}$$

Conversion ratio of the QRFW buck converter is as given below.

$$V_o = FV_g = \frac{f_s}{f_o} V_g \tag{15}$$

For the minimum load, the switching frequency is selected 200 kHz. Therefore,

$$\frac{12}{48} = 200000 \cdot 2\pi\sqrt{LC} \Rightarrow \sqrt{LC} = 198 \cdot 10^{-9} \tag{16}$$

Depending on the (14) and (16), calculated resonant elements are given TABLE II.

Quantity	Value
Resonant inductor	0.85 μH
Resonant capacitor	47 nF

V. SIMULATION STUDY

Simulation study of the designed converter has been performed in PSIM simulation software. Fig. 11 shows the simulation circuit.

For the closed loop operation, a voltage controlled oscillator is needed to control circuit but this type of a control block is not present in software library. To obtain close loop operation

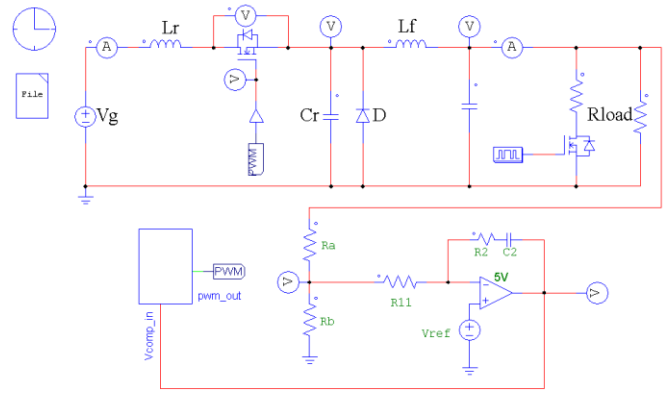


Fig. 11. Simulation circuit

result in simulation, this type of controlled must be designed.

In the designed controller, principle of a capacitor’s linear charging with a constant current is used. The capacitor is charged with a constant current source. Then, when the capacitor voltage exceeded a pre-defined limit, another current source starts to discharge capacitor and so capacitor voltage decreases linearly. Second current source is a voltage controlled current source so that a compensating voltage in the output of the closed loop error amplifier will be controlling discharge current of the capacitor.

If the voltage on the capacitor is compared with a constant DC voltage, a desired PWM will be obtained. Frequency of this PWM can be controlled with discharge current. In a ZCSHW buck converter, a frequency controlled fixed on time PWM signal is needed to control output voltage. Although variable frequency is obtained by the described method, on time of the controlled is still varies along frequency. Fig. 12 shows capacitor voltage with reference voltage and PWM signal. As shown in figure, only positive slope of the triangular capacitor voltage must be compared with reference voltage.

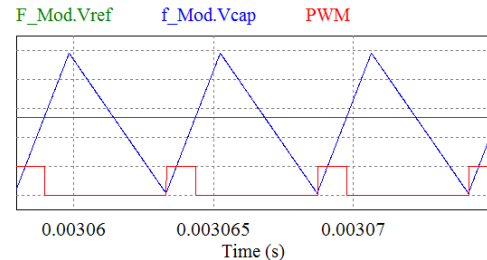


Fig. 12. Controlled capacitor voltage with reference voltage and PWM signal

To compare reference voltage with positive slope only, positive slope on the capacitor voltage must be detected. Derivative of the capacitor voltage will give the slope value. If the derivative of the capacitor voltage is positive, this means capacitor is charging. To use only sign not the value of this derivative, upper and lower limit block is used. Positive derivative gives high signal, and negative derivative gives low signal. The reference and capacitor voltage are compared, and so a signal is generated when reference is higher than capacitor voltage. The output signal is generated with given to AND integrated circuit of obtained signal and a signal of derivative slope. As a result, a fixed on time and variable

frequency PWM signal is obtained where frequency of the signal is controlled with input voltage.

Resonant tank waveforms obtained from simulation study is shown in Fig. 13. Obtained waveforms are completely matching the theoretical analysis.

MOSFET drain source voltage versus drain current which is equal to resonant inductor current is shown in Fig. 14. In the turn-on process of the MOSFET, collision between this current and voltage is very small due to series inductor; hence turn-on switching losses are very small. In the turn-off process of the MOSFET, there are no collisions between voltage and current, so switching loss at turn off process is zero.

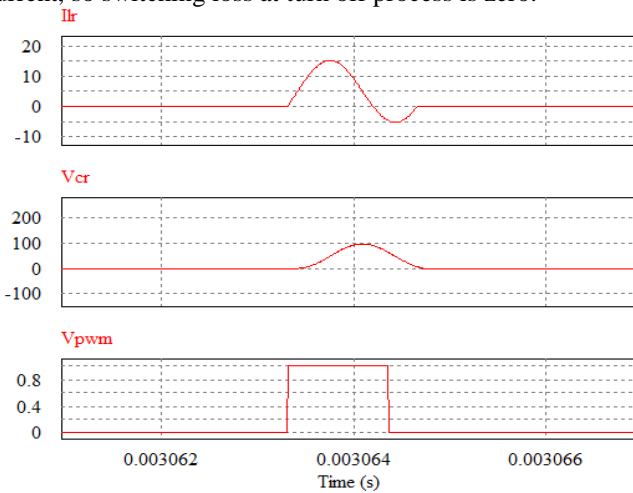


Fig. 13. Resonant tank waveforms and corresponding control signal

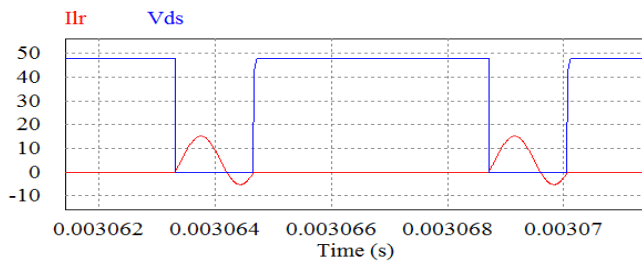


Fig. 14. MOSFET voltage versus MOSFET current

Fig. 15 shows compensated output voltage corresponding to change in output current. As can be seen in the figure, whenever output current changes from half load to full load or from full load to half load, output voltage is settles back the desired value after a small drop or a small overshoot.

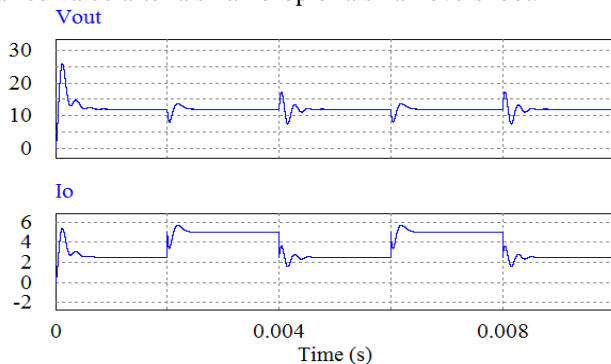


Fig. 15. Output voltage corresponding to step change in output current

VI. EXPERIMENTAL RESULTS

In this section experimental results are given and discussed. Fig. 16 shows oscilloscope plot of the inductor current and V_{DS} voltage on MOSFET. A very high frequency ringing on MOSFET voltage can be seen in the plot. This ringing occurs when MOSFET turns off due to the resonant between MOSFET's parasitic capacitor and resonant inductor. Resonant inductor current increases further than expected in positive direction after negative ringing in resonant tank.

To prevent this parasitic ringing, a RC snubber is added to the circuit. Fig. 17 shows the inductor current and V_{DS} voltage on MOSFET after the RC snubber. As it is seen in the figure, the parasitic ringing is eliminated with the RC snubber. Resonant inductor current, capacitor voltage and MOSFET gate signal is shown in Fig. 18.

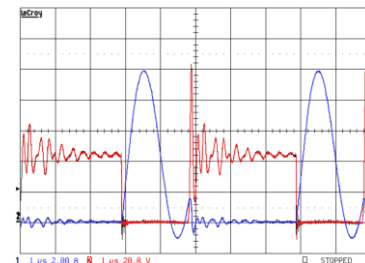


Fig. 16. Inductor current and V_{DS} voltage of MOSFET

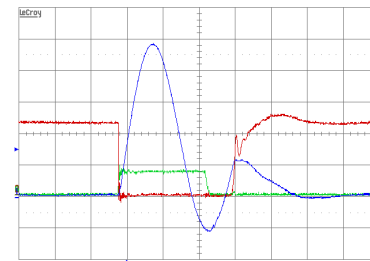


Fig. 17. Inductor current, V_{DS} voltage after the RC snubber and MOSFET gate signal

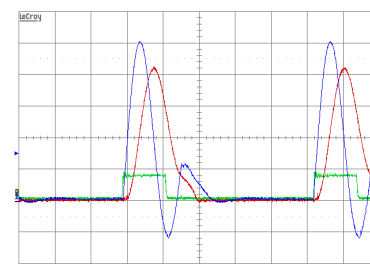


Fig. 18. Resonant capacitor voltage, resonant inductor current and MOSFET gate signal

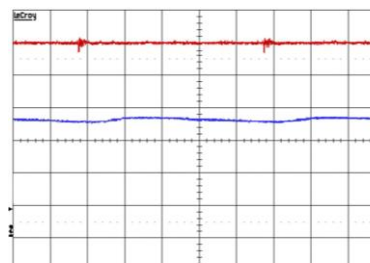


Fig. 19. Output voltage and current

Output voltage and current for open loop operation can be seen in Fig. 19. Closed loop operation of the converter for a positive step in the output current is shown in Fig. 20. After output current rises from half load to full load, output voltage drops for a short time and settles back to desired level. Output voltage response to a negative step in output current is shown in Fig. 21. Output voltage overshoots for a short period of time then settles back to desired level after change in the output current.

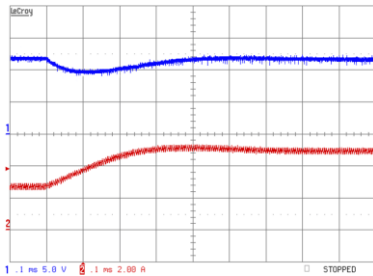


Fig. 20. Output voltage corresponding to positive step in output current

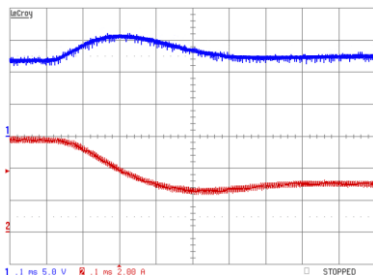


Fig. 21. Output voltage corresponding to negative step in output current

Change in the resonant inductor current for a positive step in output current is shown in Fig. 22 and for a negative step in output current is shown in Fig. 23.

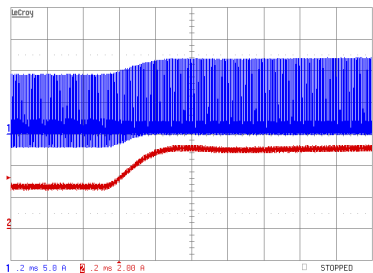


Fig. 22. Resonant inductor current change corresponding to positive step in output current

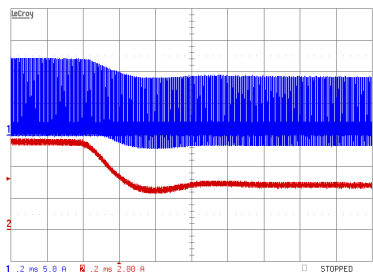


Fig. 23. Resonant inductor current change corresponding to negative step in output current

VII. CONCLUSION

In this study, a 60 W quasi-resonant full-wave zero-current switching buck converter design, simulation and experimental results are given. Although all unwanted parasitic effects on waveforms, desired result is obtained with the experimental setup. Output voltage can be controlled with switching frequency and a well filtered DC voltage with desired value can be obtained in output. Converter can regulate output voltage when the load current changes. Measured efficiency of the experimental setup is around %85. Resonant elements are crucial for a quasi-resonant converter. For a switching frequency around 200 kHz, resonant tank elements are very small, and so it is very hard to measure these elements with a LCR meter. Measurement error and a small change in this element's values, due to the external factors such as temperature, may cause major problems in operation of the converter. PCB design of such a converter has a major effect in operation. High frequency effects on every element must be considered during PCB design process. An air inductor is used for the resonant inductor. Although expected result has been obtained, the effects of an air inductor, such as EMI, should be investigated.

REFERENCES

- [1] Y.C. Chuang, Y.L. Ke, H.S. Chuang and Y.S. Wang, "A Novel Single-Switch Resonant Power Converter for Renewable Energy Generation Applications", *Industrial & Commercial Power Systems Technical Conf.*, May, 2013, pp. 1-9.
- [2] C.J. Tseng and C.L. Chen, "Novel ZVT-PWM converters with active snubbers", *IEEE Trans. on Power Electronics*, Vol. 13, Iss. 5, pp. 861-869, 1998.
- [3] D.S. Gautam and A.K.S. Bhat, "A Comparison of Soft-Switched DC-to-DC Converters for Electrolyzer Application", Vol. 28, No. 1, pp. 54-63, 2013.
- [4] I.H. Baci and S. Lungu, "Resonance in Power Converters Circuits", *IEEE 18th Int. Symp. For Design and Tech. in Electronic Packing*, Oct. 2012, pp. 183-187.
- [5] S. Urgun, "Zero-voltage transition-zero-current transition pulsewidth modulation DC-DC buck converter with zero-voltage switching-zero-current switching auxiliary circuit", *IET Power Electronics*, Vol. 5, Iss. 5, pp. 627-634, 2012.
- [6] E. Jayashree and G. Uma, "Analysis, design and implementation of a quasi-resonant DC-DC converter", *IET Power Electronics*, Vol. 4, Iss. 7, pp. 785-792, 2011.
- [7] T. Mishima and M. Nakaoka, "A Practical ZCS-PWM Boost DC-DC Converter With Clamping Diode-Assisted Active Edge-Resonant Cell and Its Extended Topologies", *IEEE Trans. on Industrial Electronics*, Vol. 60, No. 6, pp. 2225-2236, 2013.
- [8] L. Jiang, C.C. Mi, S. Li, C. Yin and J. Li, "An Improved Soft-Switching Buck Converter With Coupled Inductor", Vol. 28, No. 11, pp. 4885-4891, 2013.
- [9] N.N. Goryashin and A.S. Solomatova, "Analysis of MOSFET Operating in Half-Wave Zero-current Switching Quasi-resonant Converter", *XIII Int. Conf. and Seminar on Micro/Nanotechnologies and Electron Devices*, July 2012, pp. 333-337.
- [10] R.W. Erickson and D. Maksimovic, "Fundamentals of Power Electronics", Springer Press, 1997.



G. YANIK was born in Istanbul, Turkey, in 1985. He received his B.S. and M.S. degrees in Electrical Engineering at Yildiz Technical University, Istanbul, in 2008 and 2011, respectively.

He is a Research Assistant in the Department of Electrical Engineering, Yildiz Technical University since 2008.

His research interests include DC-DC converters, soft-switching techniques, power factor correction and inductor design.



E. ISEN was born in Bandırma, Turkey, in 1981. He received his B.S., M.S. and Ph.D. degrees in electrical engineering at Yildiz Technical University, Istanbul, in 2003, 2005 and 2012, respectively.

He was a Research Assistant in the Department of Electrical Engineering,

Yildiz Technical University between 2005 and 2012. He is an Assistant Professor in the Department of Electrical and Electronics Engineering, Kırklareli University. His current research interests include grid connected inverters, renewable energy conversion systems and power electronics.